

INVESTIGATION OF POSSIBILITY OF FIBER SPLITTING OF BICOMPONENT MELTBLOWN FIBERS BY HYDROENTANGLEMENT

Christine (Qin) Sun, Dong Zhang, and Yanbo Liu
Textiles and Nonwovens Development Center (TANDEC)
The University of Tennessee
Knoxville, TN

Abstract

Meltblowing is a most versatile and cost effective process commercially available world-wide to produce microfiber non-wovens in one step from thermoplastic resins. In recent few years there has been a growing interest in development of bi-component (bico) meltblown nonwovens. Various bicomponent pairs of meltblown fiber webs were successfully produced on Reicofil[®] bicomponent (bico) meltblown line at TANDEC since its installation in March 1999.

The bicomponent structure of microfine side-by-side meltblown fibers provided new possibility to make the finer fibers by potential fiber splitting. Two approaches of post-treatment were applied towards this investigation — mechanical and chemical methods. The mechanical method is intended to split each component apart in a side-by-side bico fiber, normally using hydroentanglement, which utilized a pressurized stream of water to split the multi-component conjugate fibers. In this paper, hydroentanglement was applied to eight bico webs including PP/Nylon 6, PET/Nylon 6, PP/PE, PET/PP, PE/Nylon-6. The web structure was extensively examined by optical microscope, and SEM. The web properties before and after the treatments were also evaluated, including basis weight, fiber diameter, bulk density, air permeability, tensile properties, and flexural rigidity.

Introduction

The concept of meltblowing thermoplastics to form microfibers (<10 microns) was first demonstrated back in 1954 by Van A. Wentz, of the Naval Research Laboratories to collect radioactive particles in the upper atmosphere to monitor worldwide testing of nuclear weapons. But it was not commercialized until 1970's the Esso Research and Engineering Co. (now ExxonMobil Chemical Co.) patented and then licensed the meltblown technology [Buntin, et al., 1976; Anonymous, 1989]. A number of companies obtained the licenses and moved quickly into commercial production since then. In May 1997, Exxon Chemical's Melt Blown Licensing Business was sold to The University of Tennessee Research Corporation (UTRC).

In a conventional meltblown process, a thermoplastic, fiber-forming polymer is extruded through a linear die containing closely-arranged small orifices (normally, about 0.4mm in orifice diameter, 20-30 holes per inch). The melt filaments out of the orifices are rapidly attenuated by two convergent streams of high-velocity hot air to form microfine fibers (usually 2-5 μm) and blown by the air stream to a collector to form the web by self-thermal bonding. Meltblowing or meltblown process (MB) has become an important industrial technique in nonwovens because it is versatile and cost-effective to produce fabrics of microfiber structure directly from polymers, suitable for filtration media, thermal insulators, battery separators, oil absorbents, etc.. Polypropylene (PP) is the most widely used polymer for this process. Many of others such as polyethylene (PE), polyethylene terephthalate (PET), polybutylene terephthalate (PBT), polyamide (PA), polytrimethylene terephthalate (PTT) can also be used to produce the meltblown webs. Each material has its characteristic advantages and disadvantages vis-à-vis the properties desired in the final product to be made from such fibers.

The term "bicomponent" usually refers to fibers which are formed by two polymers extruded separately from at least two extruders but spun together to form one fiber. The configuration of such a bicomponent fiber may be a sheath/core arrangement wherein one polymer is surrounded by another or may be a side-by-side or other sectional configurations. In nonwovens industries, the bicomponent (bico) fibers have been obtained in the recent years for the meltblown and spunbond processes. The first Reicofil[®] side-by-side bicomponent meltblown line was started up at the University of Tennessee's Textiles and Nonwovens Development Center (TANDEC) in March 1999.

Various mono and bicomponent meltblown web samples were produced on the bico meltblown line at TANDEC using PP, PE, PET, PBT, PA6, PTT, etc., and their bico pairs such as PP/PE, PET/PE, PBT/PP, PA6/PP, PBT/PP, PTT/PP at bico weight ratios of 25/75, 50/50, and 75/25 [Zhang, et al., 1999 and 2000; Sun, et al., 2000]. The fact that side-by-side bico fiber structure was achieved opened the door to many exciting possibilities, such as enhanced barrier properties, more resilient curly meltblown fibers, etc. Among these there is a continuing quest to obtain even finer meltblown fiber nonwovens by splitting the side-by-side fibers.

Two approaches of post-treatment were applied at TANDEC to pursue the fiber splitting — mechanical and chemical methods. The mechanical method was intended to split each component apart in a side-by-side bico fiber using hydroentanglement, which utilized a pressurized stream of water to split the multi-component conjugate fibers. For chemical treat-

ment, substantial portion of the conjugate fibers was removed by a dissolving process and the un-dissolvable part remained in the fibers.

In this paper, efforts were made to explore possibility of the fiber splitting by hydro-entanglement. The web structure and properties before and after the post-treatment were also studied.

Experimentals

Web Preparation I

Eight bico meltblown webs were produced with TANDEC Refenhäuser 24" wide Bico Meltblown Line in February 2001, with PP of ExxonMobil 3546G, PE of Dow 6808A, PET of Wellman, PBT of Ticona Celanex 1300A, PTT of Shell VFR 50009. The die air gap and setback were 0.8mm and 1.0mm, respectively. Table 1 gives the processing conditions for the meltblown webs of 75PP/25PE, 50PP/50PE, 25PP/75PE, 75PET/25PTT, 50PET/50PTT, 25PET/75PTT, 75PTT/25PBT, 50PTT/50PBT.

Hydroentanglement I

The webs shown in Table 1 were hydro-entangled at Fleissner Inc., Germany in a format of Side A-Side B-Side A-Side B. The machine setting was as follows:

Step 1	(drum, 100 mesh)	Step 2 (drum, 100 mesh)
	Injector 1: 30 bar	Injector 3: 120 bar
	Injector 2: 60bar	
Step 3	(drum, 100 mesh)	Step 4 (belt, 120 mesh)
	Injector 4: 120 bar	Injector 5: 120 bar

Web Preparation II

Eight nylon-based bico webs were produced to further explore the possibility of the fiber splitting by the pairs of PP/Nylon 6, PE/Nylon 6, PET/Nylon 6. BASF B3 Nylon 6, ExxonMobil 3155 PP, Dow 6808A PE, and Wellman PET resins were applied. Table 2 lists the web description and processing conditions on the bico line.

Hydroentanglement II

The webs in Table 2 were also hydro-entangled at Fleissner Inc., Germany. But three levels of water jet pressure were applied for each sample, 80 bar, 100 bar and 120 bar.

Web Characterization

The web test included basis weight, bulk density, fiber diameter (SEM), air permeability (ASTM D 737), tensile properties (ASTM D 1117), flexural rigidity (ASTM D 1338-64) and hydrostatic head (IST 80.4-92). In addition, Microscope and SEM (Scanning Electrical Microscope) were also applied to examine the web structure. An image analysis software called Webpro developed at TANDEC was used to measure the web uniformity.

Web Uniformity Analysis

Weight uniformity has traditionally been used as a quality index for nonwoven webs. Physical, mechanical and aesthetic properties of the webs, as well as variation in web performance, are known to be influenced by the uniformity of web structure, which was measured by an optical microscope driven by an image analysis software Webpro at TANDEC. This software utilizes various measures of optical uniformity and is able to evaluate several different types of structural uniformity. Web uniformity actually analyzes the optical property. However, both theory and experiments showed that web basis weight was linearly related to optical intensity. Optical and weight uniformities were in excellent agreement and required no corrections. Uniformity spectra provide information about web uniformity at different size resolution, and were demonstrated to be useful for providing detailed uniformity information for webs. The CV% of small cell size was associated with microscopic structural uniformity whereas the CV% of large cell size was associated with macroscopic structural uniformity [Huang and Bresee, 1993]. A total of 256 images were randomly selected to evaluate the web uniformity in this test.

Results and Discussion— Set I

Figure 1 gives the basis weight of the bico samples in Set I before and after hydroentanglement. Interestingly, basis weight showed slightly decrease for the PP/PET and PBT/PTT bico webs, which might result from the fiber loss during the post-treatment. It did not show apparently change trend for the PP/PE bico webs.

Figure 2 shows the fiber diameter of Set I webs before and after hydroentanglement. Most samples showed a slightly decrease in fiber diameter after hydroentangling. Figure 3 are four SEM pictures of two bico webs before and after hydroentanglement. No fiber splitting was detected after hydroentanglement for the webs in Set I. The minor change in fiber diameter might be due to the test error.

The SEM observation showed that the fibers did not effectively split by the hydroentanglement for the bico pairs PP/PE, PP/PET and PTT/PBT in Set I. Hydroentanglement is currently the most widely used method to split multi-component fiber mechanically. But it did not successfully used to produce split the bico meltblown fibers. The reason might be due to insufficient pressure of the water jets or the relatively too strong interfacial adhesion in the bico fibers. The autogenously bonded meltblown fiber structure, which have very fine breakable fibers and contain substantially uniformly distributed numerous interfiber bonds that restrict fiber movements, are difficult to split with the regular mechanical splitting process.

The bulk density increased after the hydroentanglement (Figure 4). The results were consistent to the more compact appearance of the web after the hydroentanglement. The post-treatment increased the strength for PP/PET and PBT/PTT bico webs, but showed an opposite trend for the strength of the PP/PE bico webs (Figure 5).

The breaking elongation did not show consistent trend. The decreasing tenacity did resulted in increasing breaking elongation, such as PP/PE bico webs, and vice versa. Air permeability decreased (Figure 7) due to the more compact fiber structure after the treatment, which also resulted in increased hydrohead in Figure 8.

Figure 9 shows that the hydroentanglement reduced flexural rigidity of the webs and notably improved their softness. The hydroentangling processes made the webs softer but more compact and more water-resistant.

Results and Discussion— Set II

The motivation of research on Set II was to further explore the possibility of bico MB fiber splitting by using various and more incompatible bico pairs such as PET/PA6. Three different levels of water jet pressure were applied to each sample in Set II for the hydroentangling process. Basis weight, fiber diameter, bulk density, tenacity, breaking elongation, air permeability, hydrohead and flexural rigidity were evaluated similarly to the samples in Set I. The results are showed in Figures 10-17.

Different from the results obtained for Set I, the webs apparently shrunk and the basis weight increased after the treatment (Figure 10). An exception happened to PET/PA6 web, indicating that the fibers were too loose in web and had some lost during the hydroentangling process.

The fiber size was notably decreased (Figure 11). Fiber splitting was detected after the hydroentanglement by SEM (Figure 12). To comprehensively understand the structure of the bico webs before and after the treatment, SEM observations were extensively conducted and more SEM pictures are attached in Appendix 3. It appeared that more fiber breakage than fiber splitting occurred during the hydroentangling process, which indicated that the bico meltblown fibers might be too weak to achieve the overall fiber splitting by the mechanical method.

The bulk density did not show consistently changing trend by the hydroentanglement as it did in Set I (Figures 4, 14). It generally increased, but 25PE/75PA6 and 25PET/75PA6 bico webs exhibited decreasing bulk density after the hydroentanglement, indicating that the bulkier web structure might resulted from the fiber splitting.

Air permeability and hydrohead showed an opposite trend compared to those in Set I (Figures 7, 8, 17, 18). Air permeability increased but hydrohead significantly decreased after the hydroentanglement. It was also noted that as the water pressure changed from 80 bars, to 120 bars, air permeability increased and hydrohead decreased.

Interestingly, the web extension was significantly increased for all the samples in Set II after hydroentanglement (Figure 16). But for the tenacity, it did not show consistent trend as did the webs in Set I (Figure 15). The web strength of 50PA/50PET and 75PA/25PET was dramatically improved by hydroentanglement since the original webs were loose and very weak.

The flexural rigidity decreased a lot after the treatment (Figure 19), demonstrating the web softness was much improved. But exceptions existed for the two PET/PA6 webs since they were originally very poorly bonded during the meltblowing process and exhibited an extremely soft hand.

Figures 20-22 are the uniformity analysis results for bico 50PET/50PA6 web by using the Webpro. Figure 20 shows that the overall uniformity before and after hydroentanglement. The web after the treatment demonstrated greater variance, indicating that the web uniformity was deteriorated by the hydroentanglement. Figure 21 shows that the uniformity decreased both in the MD and CD directions. Figure 22 is the web uniformity of an original web before the treatment. The results also indicated that the web was more uniform in the MD direction than in the CD direction.

The web uniformity analysis were performed for most samples in Set II, the results were consistence as described above. The reason of uniformity deterioration by the hydroentanglement is not hard to understand by observation of Figure 23, which shows two web images under an optical microscope. One is for the web before the treatment and the other is for the web after

the treatment. The holes punched by water jets during the hydroentangling process decreased the web uniformity, which are also the reason for the increased air permeability and decreased hydrohead after the hydroentanglement.

Summary

Side-by-side bi-component meltblown fiber webs were produced on 24-inch wide Reicofil® Bico MB Line at TANDEC using PP, PE, PET, PBT, PA-6, PTT, PA6. Post-treatment of hydroentanglement was conducted to investigate the possibility of the fiber splitting. Split fibers were detected via SEM in PP/PA6, PE/PA6 and PET/PA6 bico webs after the treatment. But no split fiber was found for the webs paired by PP/PE, PP/PET and PBT/PTT. It appeared that more fiber breakage than fiber splitting occurred in the webs, indicating that the meltblown fibers might be too weak to achieve the overall fiber splitting mechanically before the breakage.

The effect of hydroentanglement varied with the processing conditions, bico composition and original web structure. The post-treatment generally increased the basis weight, bulk density and softness. The fiber size was notably decreased for the webs of split fibers including the PP/PA6, PE/PA6, PET/PA6 bico pairs. The air permeability was decreased and hydrohead was increased after the hydroentanglement for the PP/PE, PP/PET and PBT/PTT webs, but they changed in the opposite direction for the bico webs paired by PP/PA6, PE/PA6, and PET/PA6. The web uniformity analysis showed that the webs were more uniform in the MD than in the CD and the hydroentanglement deteriorated the uniformity of PP/PA6, PE/PA6, PET/PA6 bico webs.

Acknowledgement

The authors would like to thank Reifenhäuser GmbH at Troisdorf, Germany for financial support. The assistance of Fleissner, Inc. in Germany for the hydro-entangle treatment, Gary Wynn and Stanley Gredig for web preparation are greatly appreciated.

References

Anonymous, *Meltblown Technology Today*, Miller Freeman Publications, San Francisco, 1989, pp.7-12.

Buntin, Robert R., James P. Keller, John W. Harding, 'Melt blowing process' US Patent 3,978,185, Assigned to Exxon Research and Engineering, August 31, 1976.

Dugan, Jeff, 'Critical Factors in Engineering Segmented Bicomponent Fibers for Specific End-Uses', *INDA-TEC'99*, September 21-23, 1999, Atlanta, GA, USA.

Huang, Xuan-chao and Randall R. Bresee, *Characterizing Nonwoven Web Structure Using Image Analysis Technique*, Part III: Web Uniformity Analysis, *INDA Journal of Nonwovens Research*, summer 1993, Vol. 5, No.3 p28-38.

Huang, Xuan-chao and Randall R. Bresee, *Characterizing Nonwoven Web Structure Using Image Analysis Techniques*, Part II: Fiber Orientation Analysis in Thin Webs, *INDA Journal of Nonwovens Research*, Spring 1993, Vol.5, No.2. p14-21.

Krueger, Dennis L., James F Dyrud, 'Respirator comprised of blown bicomponent fibers', US Patent 4,729,371, Assigned to Minnesota Mining and Manufacturing Company, March 8, 1988.

McCulloch, John G., 'The History of the Development of Melt blowing Technology', *International Nonwoven Journal*, Spring 1999.

Sun, Christine (Qin), Dong Zhang, Larry Wadsworth, and Rongguo Zhao 'Processing Development and Investigation of Mono-and Bi-component Fiber Meltblown Nonwovens', *Proceedings of 10th TANDEC Conference*, November 6-9, 2000, Knoxville, TN, USA.

Wadsworth, Larry C., Christine (Qin) Sun, Dong Zhang and Rongguo Zhao, 'SM and SMS Laminates Produced with 100% PP Melt Blown and Bicomponent Fiber PP/PE Melt Blown Webs', *Nonwovens Industry*, December 1999.

Zhang, Dong Christine(Qin) Sun, Larry Wadsworth, and Rongguo Zhao, 'Processing and Characterization of Mono- and Bi-component Fiber Meltblown Nonwovens', *Proceedings of 9th TANDEC Conference*, November 10-12, 1999, Knoxville, TN, USA.

Zhang, Dong, Christine (Qin) Sun, and John Beard, 'Development and Characterization of Poly (Trimethylene Terephthalate) based Bicomponent Meltblown Nonwovens', *Proceedings of 10th TANDEC Conference*, November 6-9, 2000, Knoxville, TN, USA.

Table 1. Processing Conditions for Bico Sample in Set I.

Sample ID	Sample Description	Melt Temp. (°F)	Melt		Air Flow	
			Throughput (g/h/min)	Air Temp. (°F)	Rate (SCFM)	DCD (in)
I-1	50PP/50PE	500/480	0.55	480	350	8.0
I-2	75PP/25PE	500/480	0.55	480	350	8.0
I-3	75PE/25PP	500/480	0.55	480	350	8.0
I-4	75PP/25PET	580/590	0.55	600	550	10.0
I-5	50PP/50PET	580/590	0.55	600	550	10.0
I-6	25PP/75PET	580/590	0.55	600	550	10.0
I-7	75PBT/25PTT	520/520	0.73	500	520	10.0
I-8	25PBT/75PTT	520/520	0.73	500	520	10.0

Note: Air gap/Setback = 0.8mm/1.0mm
Using filtered die

Table 2. Processing conditions for Bico Sample in Set II.

Sample ID	Sample Description	Melt Temp. (°F)	Melt		Air Flow Rate (SCFM)	DCD (in)
			Throughput (g/h/min)	Air Temp. (°F)		
II-1	25PP/75PA6	590/590	0.55	600	350	8.0
II-2	50PP/50PA6	590/590	0.55	600	350	8.0
II-3	75PP/25PA6	590/590	0.55	600	350	8.0
II-4	25PE/75PA6	570/590	0.55	590	550	8.0
II-5	50PE/50PA6	570/590	0.55	590	550	8.0
II-6	75PE/25PA6	570/590	0.55	590	550	8.0
II-7	50PET/50PA6	590/590	0.73	590	520	8.0
II-8	25PET/75PA6	590/590	0.73	590	520	8.0

Note: For Samples II-(1-6), Air gap/Setback = 0.8mm/1.0mm, using filtered die
For Samples II-(7,8), Air gap/Setback = 1.5mm/1.5mm, using no-filter die

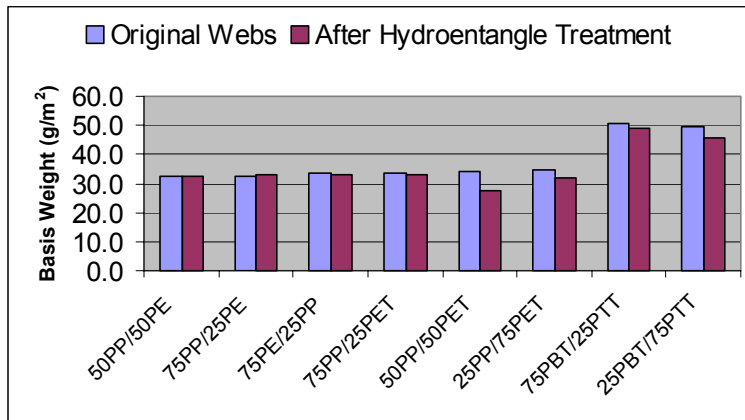


Figure 1. Basis Weight of Samples in Set I before and after Hydroentanglement.

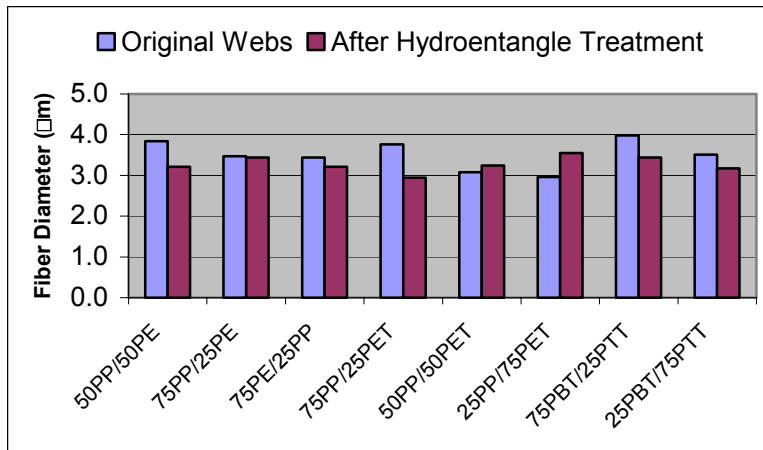
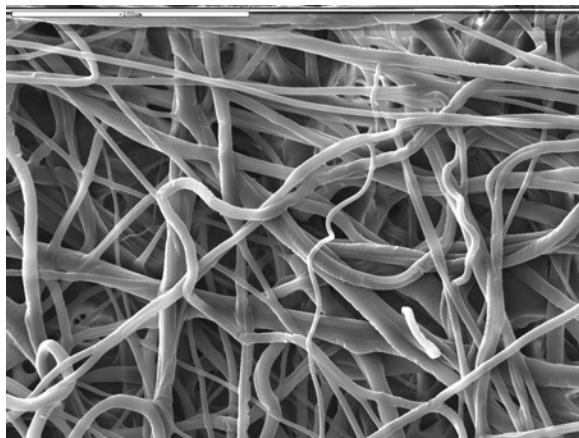
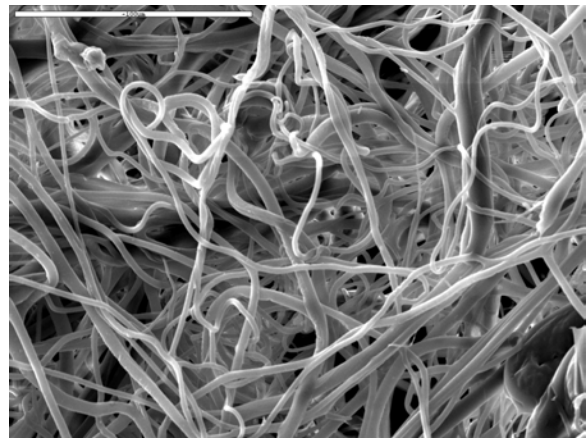


Figure 2. Fiber Diameter of Samples in Set I before and after Hydroentanglement.



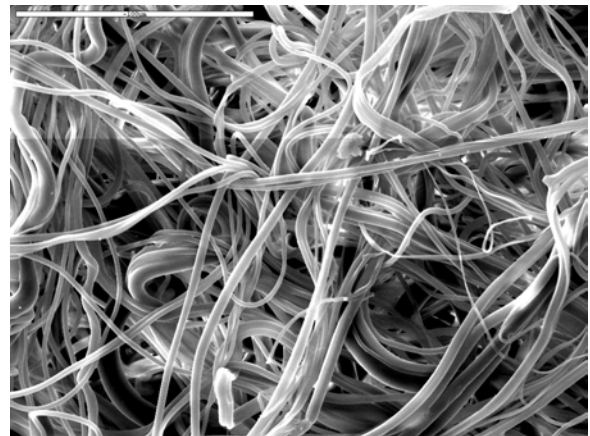
50PP/50PE (before)



50PP/50PE (after)



75PP/25PET (before)



75PP/25PET (after)

Figure 3. SEM Images of Bico webs in Set I before and after Hydroentanglement.

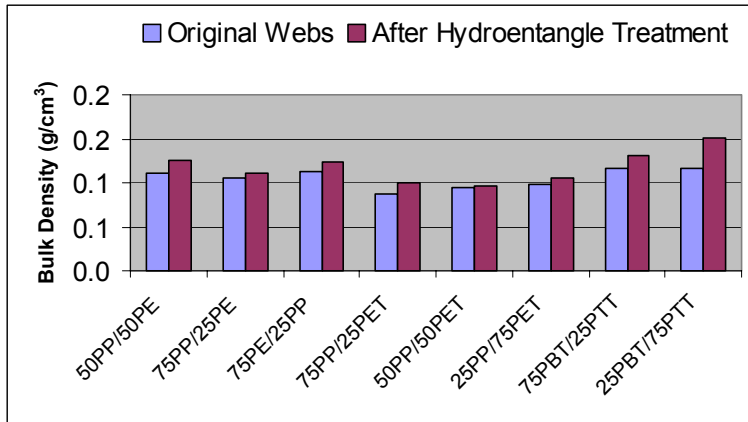


Figure 4. Bulk Density of Bico Webs in Set I before and after Hydroentanglement.

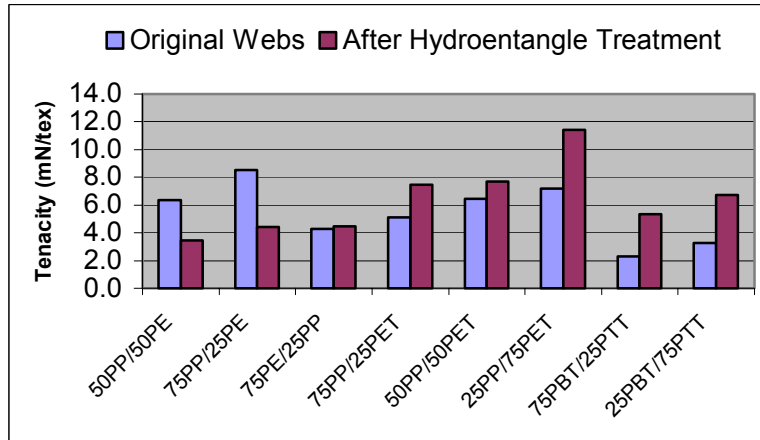


Figure 5. Tenacity of Bico Webs in Set I before and after Hydroentanglement.

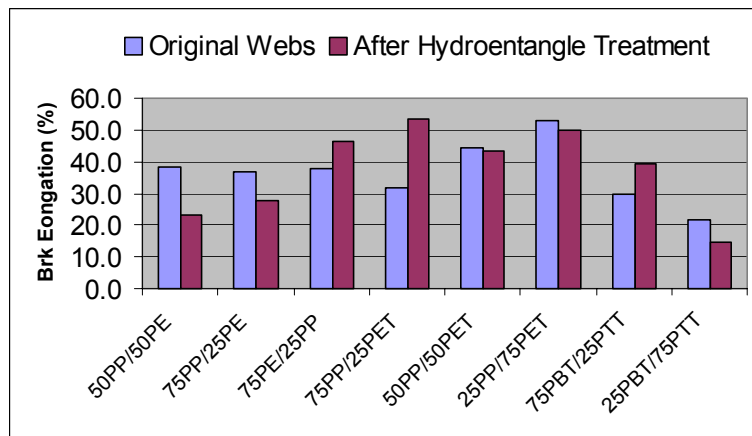


Figure 6. Breaking Elongation of Bico Webs in Set I before and after Hydroentanglement.

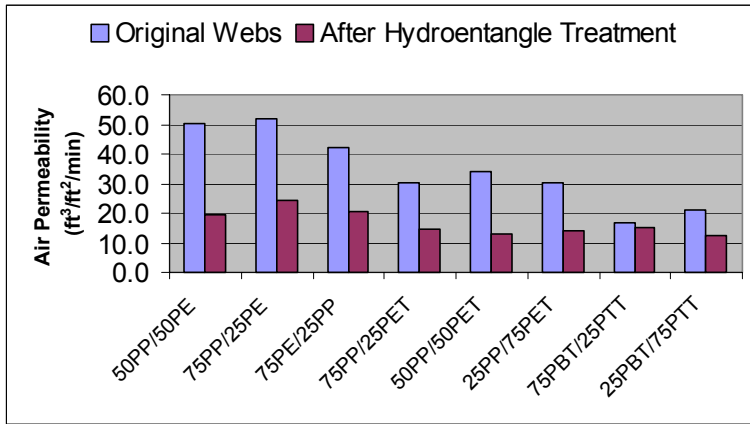


Figure 7. Air Permeability of Bico Webs in Set I before and after Hydroentanglement.

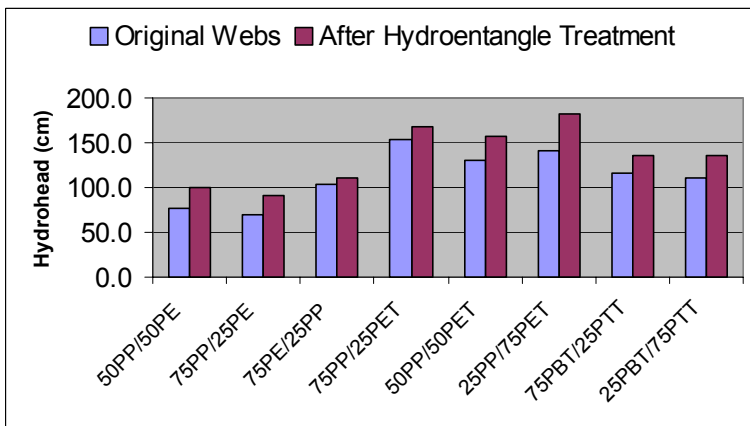


Figure 8. Hydrohead of Bico Webs in Set I before and after Hydroentanglement.

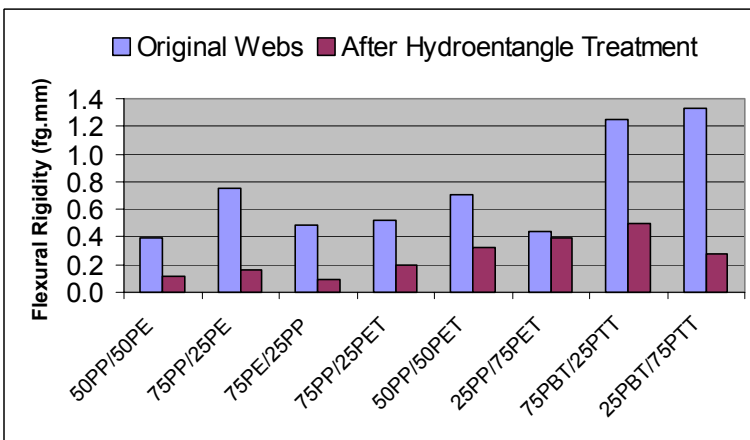


Figure 9. Flexural Rigidity of Bico Webs in Set I before and after Hydroentanglement.

■ Original
 ■ Hydroentangling (80 bar)
 ■ Hydroentangling (100 bar)
 ■ Hydroentangling (120 bar)

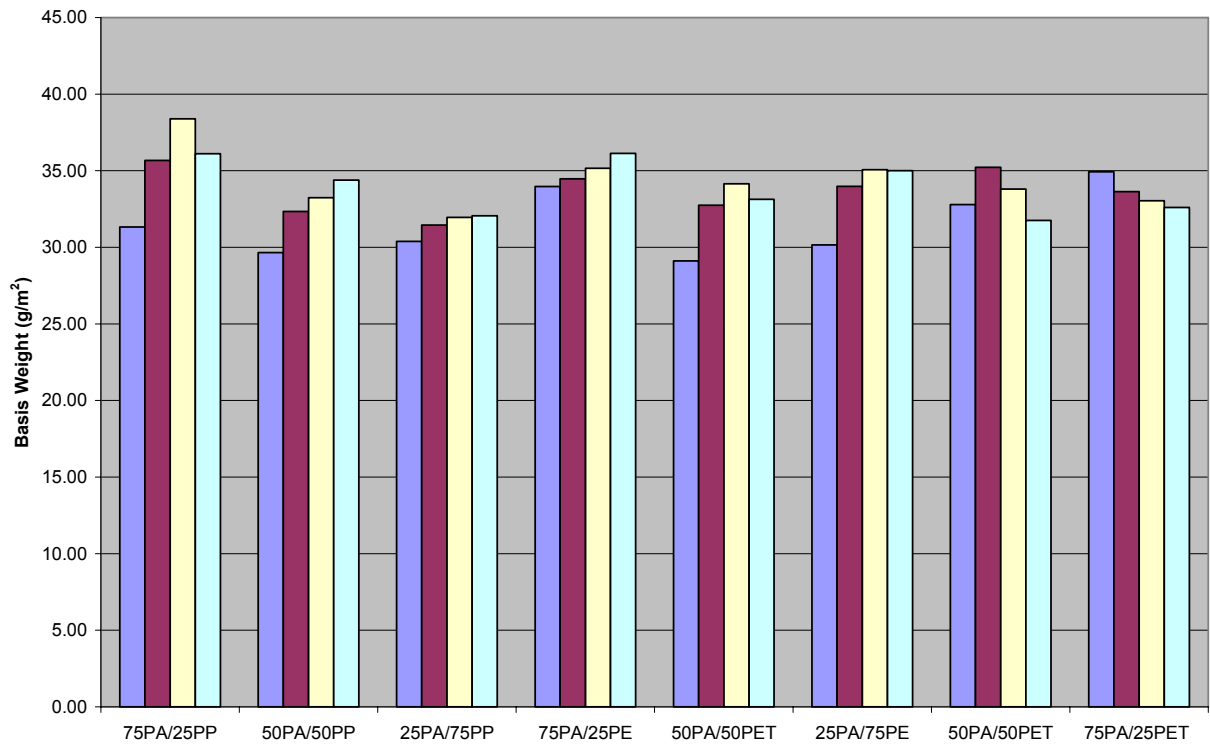


Figure 10. Basis Weight of Samples in Set II before and after Hydroentanglement.

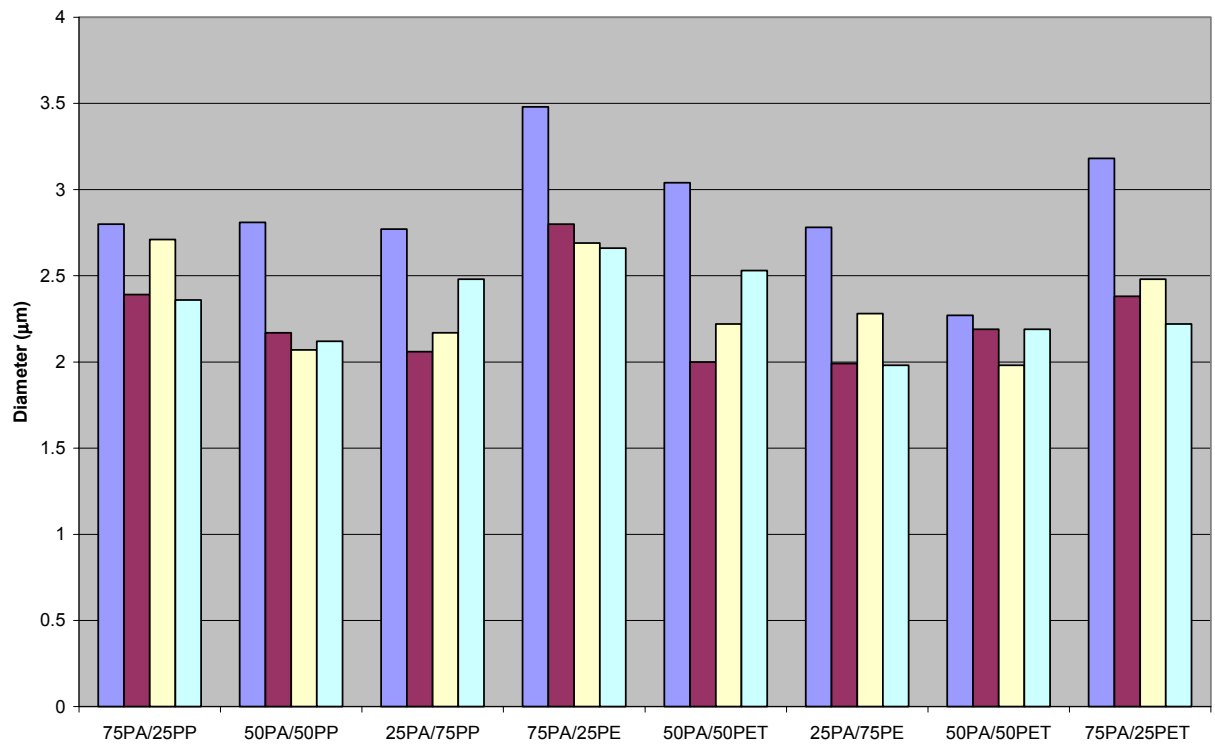
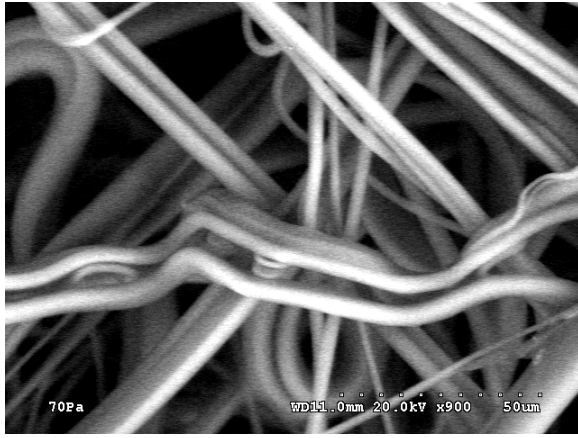
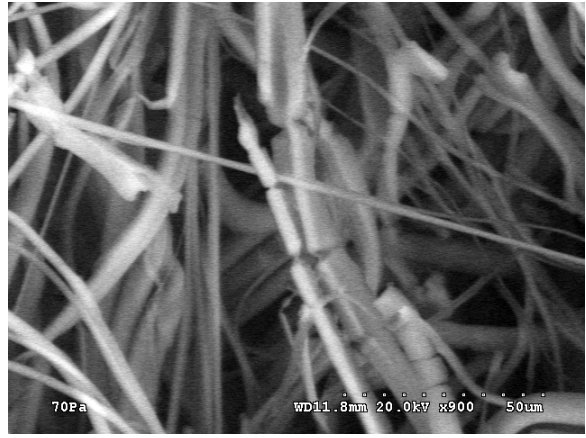


Figure 11. Fiber Diameter of Samples in Set II before and after Hydroentanglement.



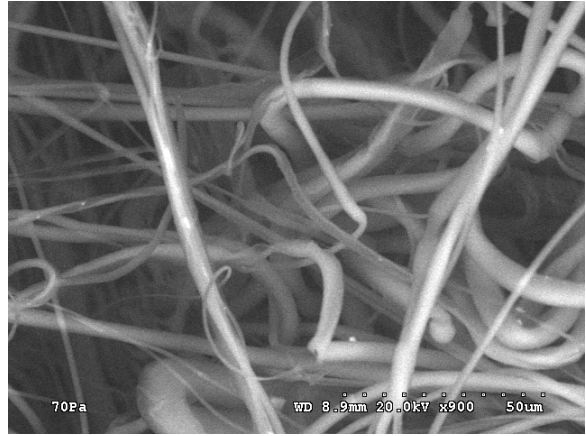
50PP/50PA (before)



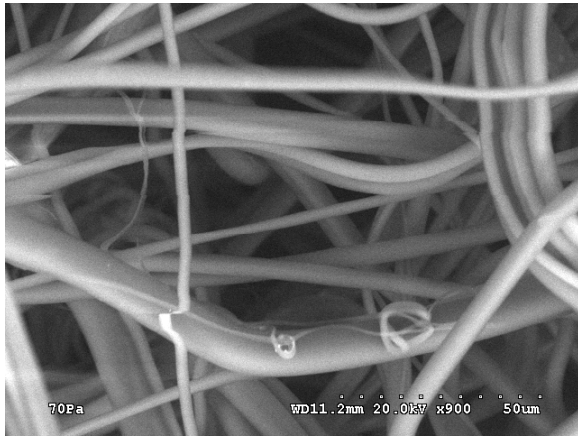
50PP/50PA (after, 80 bars)



50PE/50PA6 (before)



50PE/50PA6 (after, 80 bars)

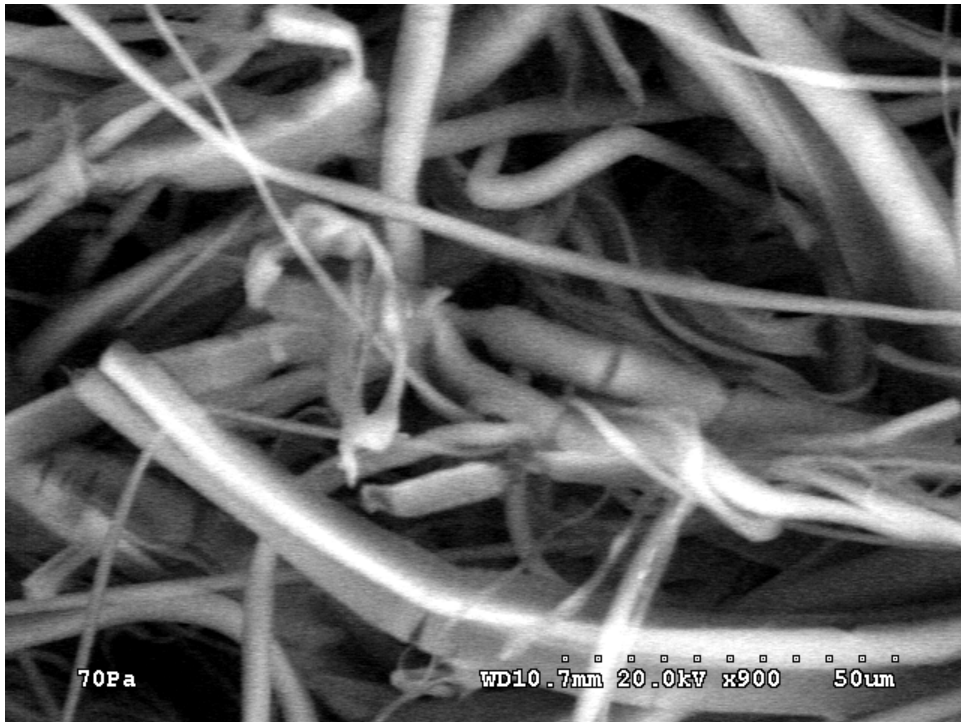


25PET/75PA6 (before)



25PET/75PA6 (after, 100 bars)

Figure 12. SEM Images of the Bico Webs Before and After Hydroentanglement II.



50PP/50Nylon6 after hydroentanglement (80 bars)



25PET/75PA6 after hydroentanglement (120 bars)

Figure 13. SEM Pictures of 50PP/50PA before and after Hydroentanglement.

■ Original
 ■ Hydroentangling (80 bar)
 ■ Hydroentangling (100 bar)
 ■ Hydroentangling (120 bar)

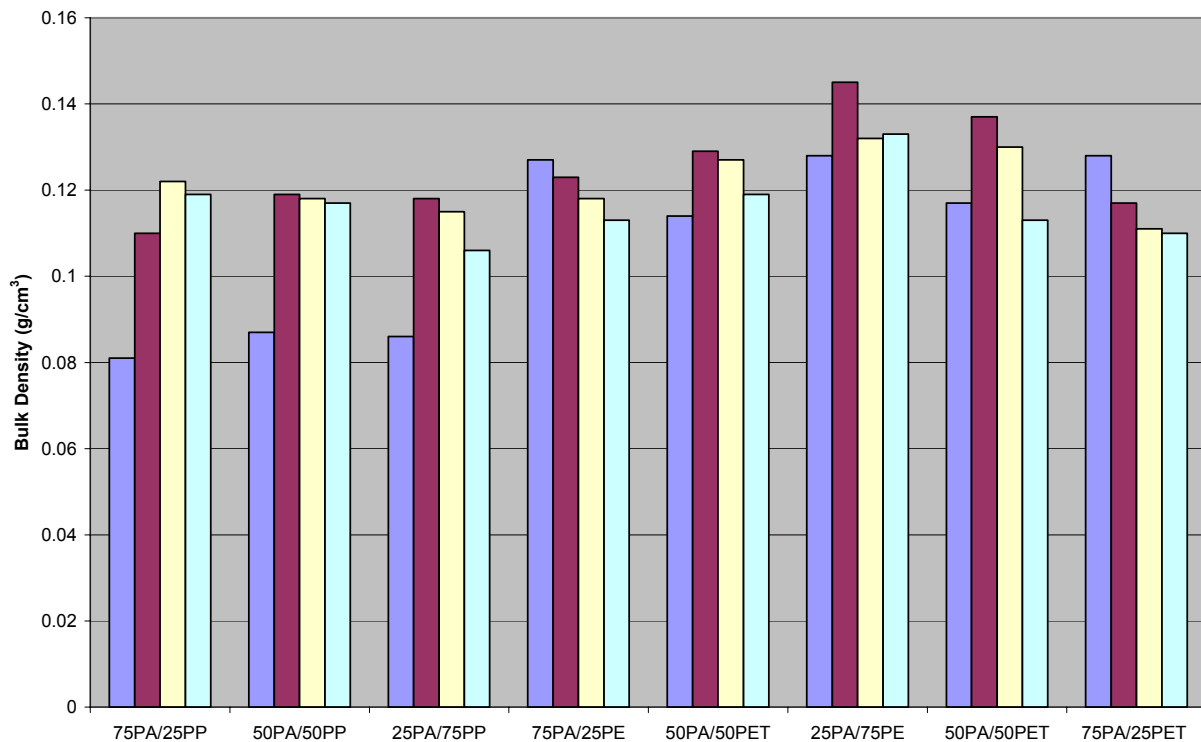


Figure 14. Bulk Density of Samples in Set II before and after Hydroentanglement.

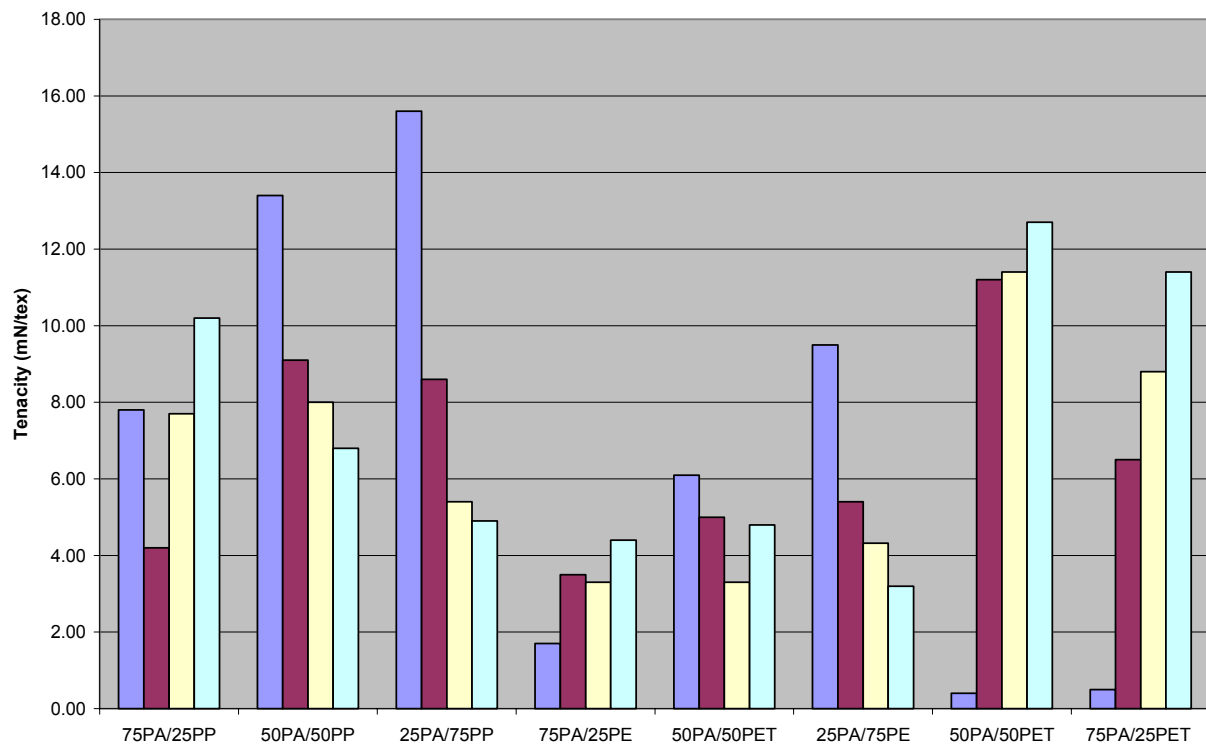


Figure 15. Tenacity of Samples in Set II before and after Hydroentanglement.

■ Original
 ■ Hydroentangling (80 bar)
 ■ Hydroentangling (100 bar)
 ■ Hydroentangling (120 bar)

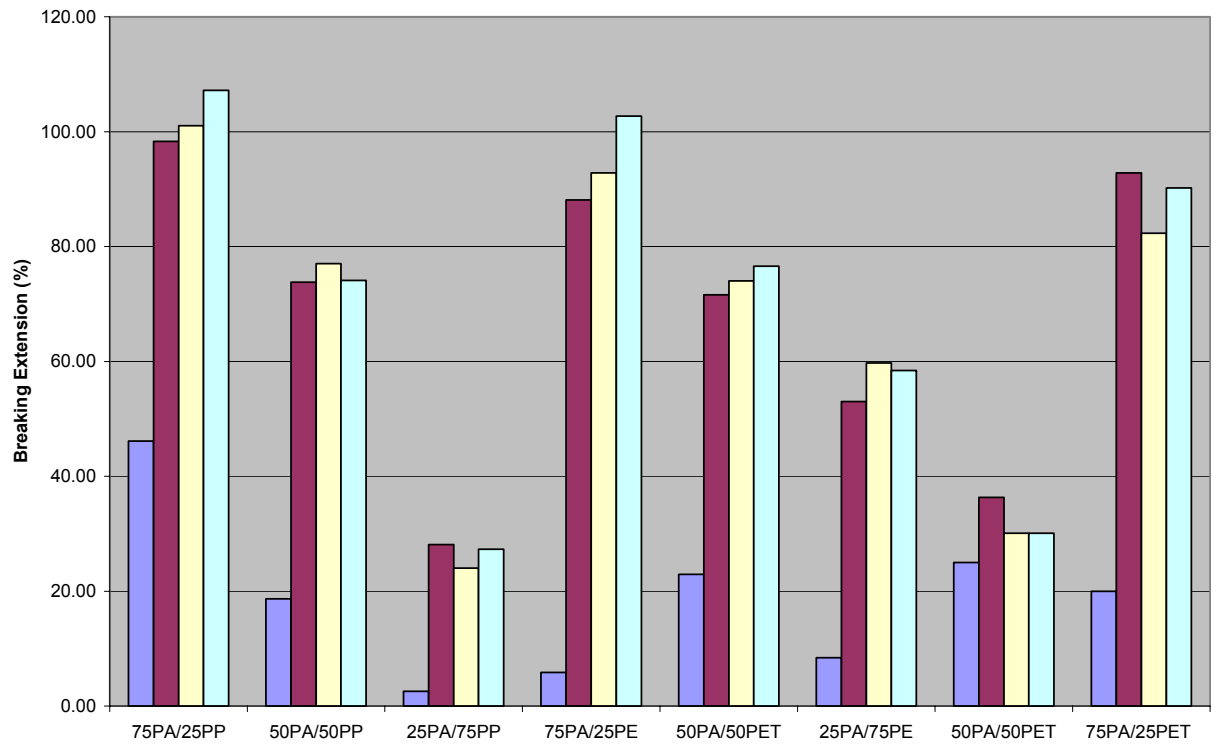


Figure 16. Breaking Elongation of Samples in Set II before and after Hydroentanglement.

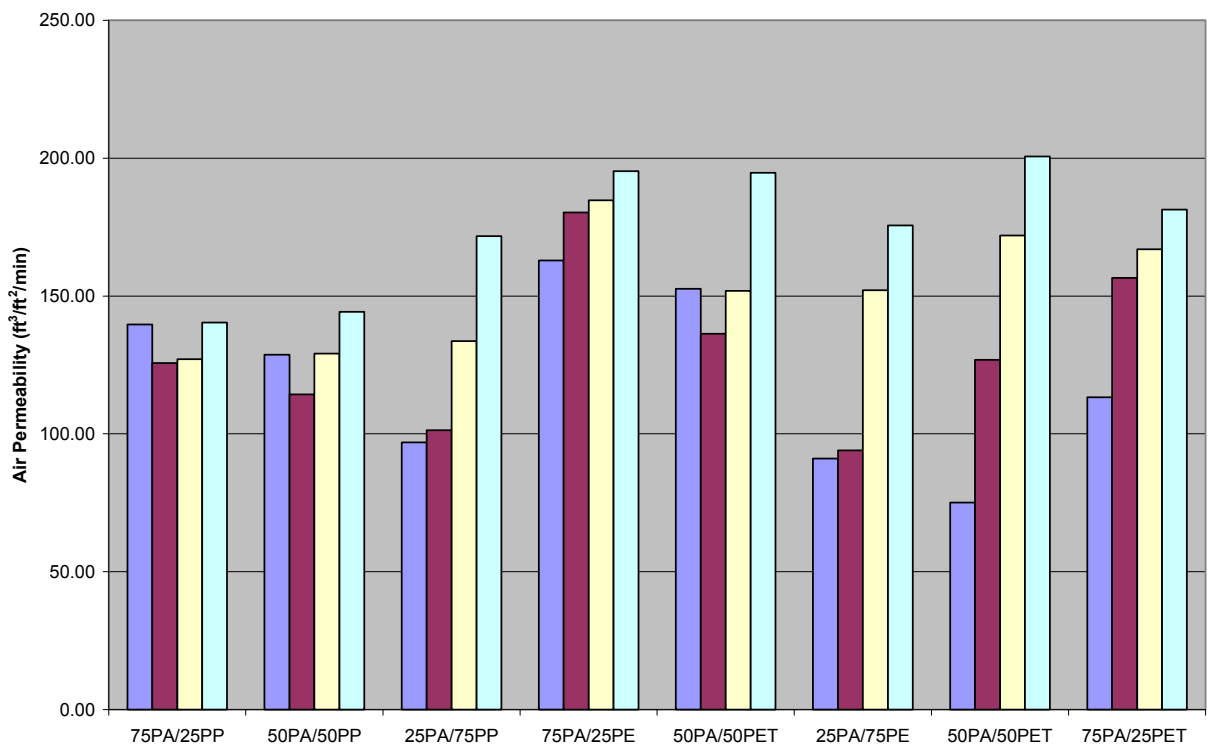


Figure 17. Air Permeability of Samples in Set II before and after Hydroentanglement.

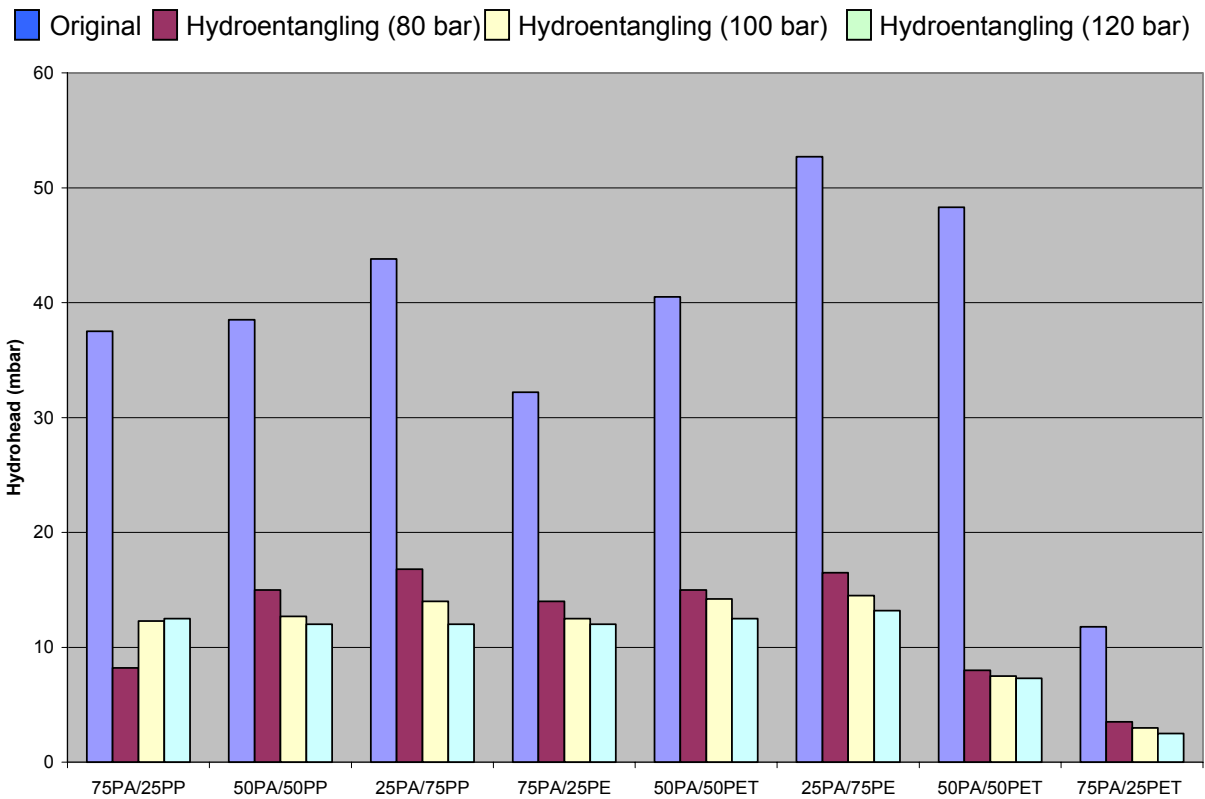


Figure 18. Hydrohead of Samples in Set II before and after Hydroentanglement.

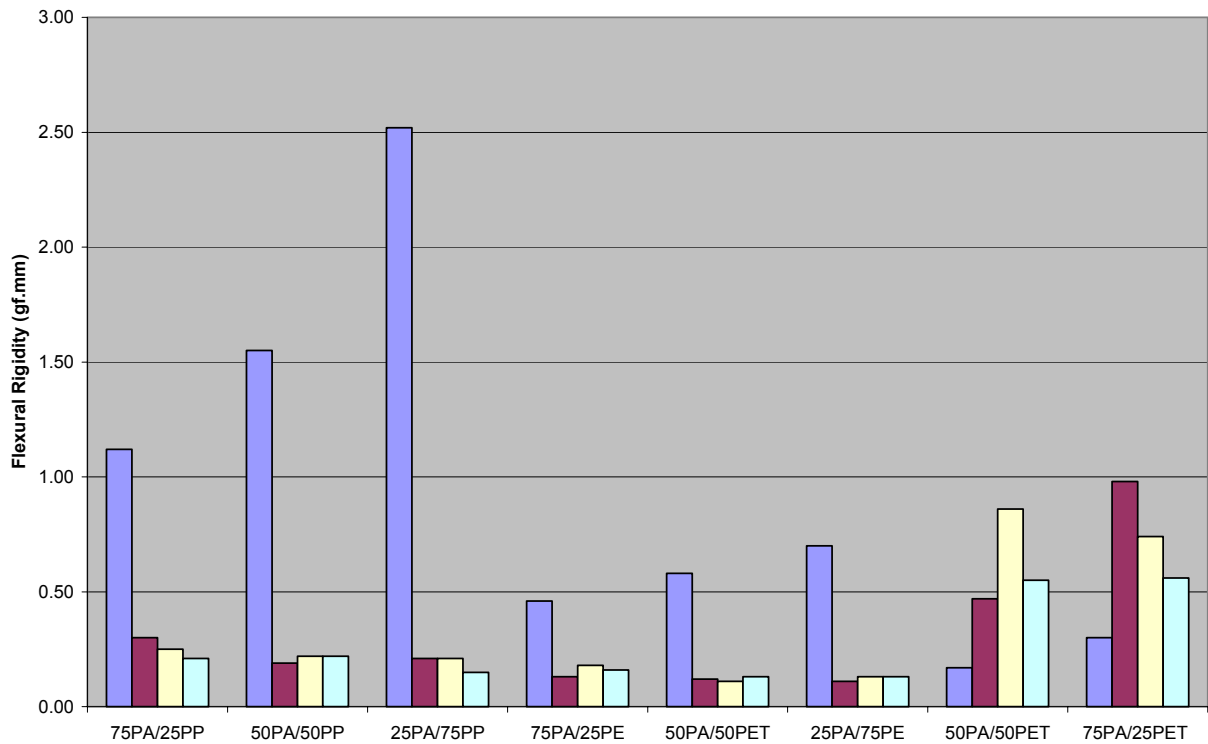


Figure 19. Flexural of Samples in Set II before and after Hydroentanglement.

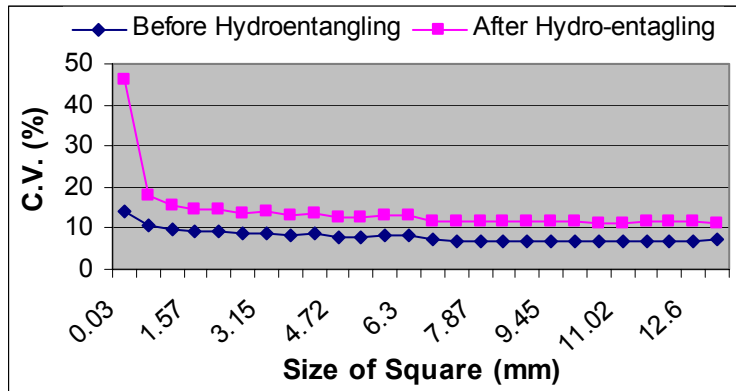


Figure 20. Overall Uniformity of the Meltblown web (50PET/50PA6) before and after Hydroentanglement.

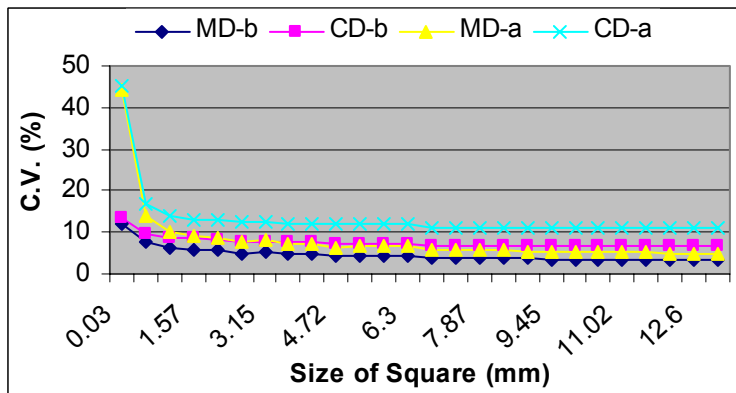


Figure 21. MD and CD Uniformity of the Meltblown Web (50PET/50PA6) before and after Hydroentanglement.

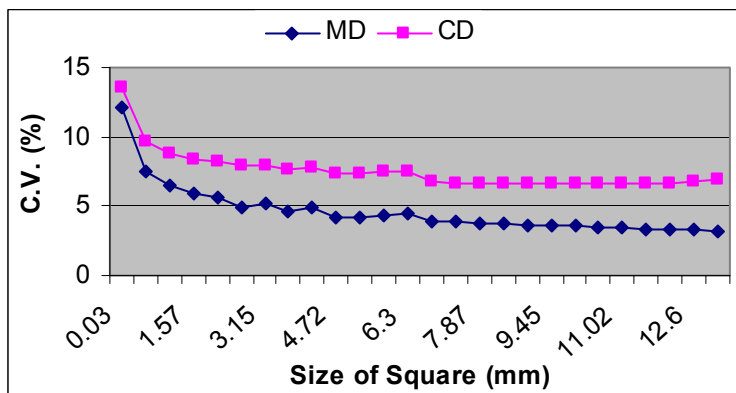
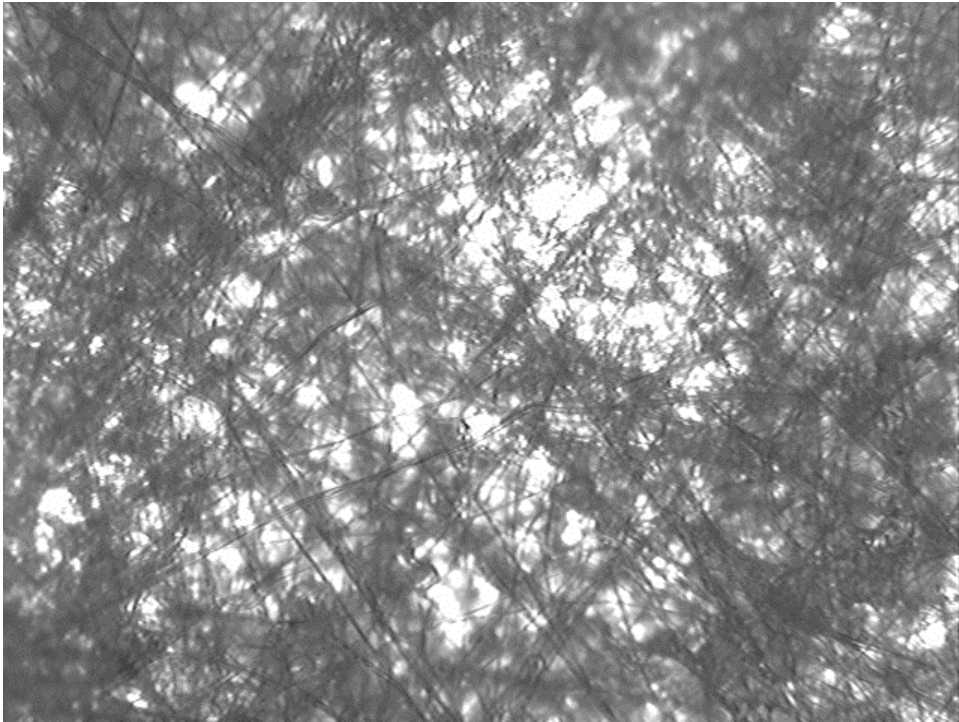
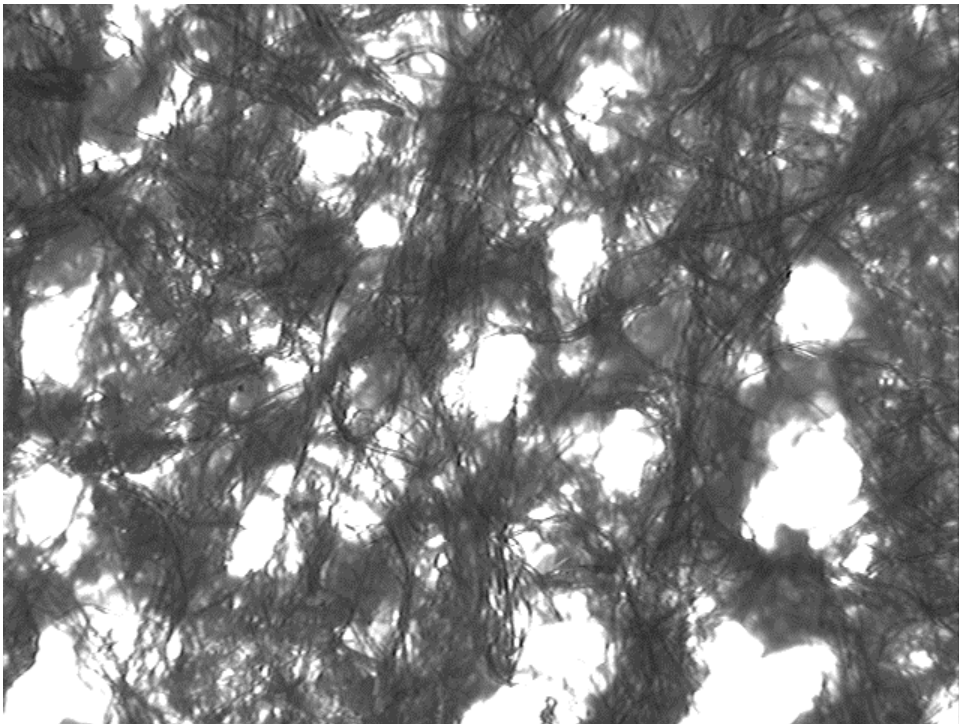


Figure 22. Uniformity of the Meltblown Web (50PET/50PA6) in MD and CD Directions (before hydroentanglement).



before hydroentanglement



after hydroentanglement

Figure 23. Optical Microscope Images for the Web (75PP/25PA6) before and after Hydroentanglement (the same magnification was used, about 80X).